

PROTEIN STRUCTURE REPORT

Crystal structure of Jararacussin-I: The highly negatively charged catalytic interface contributes to macromolecular selectivity in snake venom thrombin-like enzymes

A. Ullah,¹ T. A. C. B. Souza,² L. M. Zanphorlin,¹ R. B. Mariutti,¹
V. S. Santana,¹ M. T. Murakami,² and R. K. Arni^{1*}

¹Multi User Center for Biomolecular Innovation, Department of Physics, IBILCE/UNESP, São Jose do Rio Preto, SP, Brazil

²Brazilian Biosciences National Laboratory (LNBio), CNPEM, Campinas, SP, Brazil

Received 28 August 2012; Revised 27 October 2012; Accepted 29 October 2012

DOI: 10.1002/pro.2189

Published online 8 November 2012 proteinscience.org

Abstract: Snake venom serine proteinases (SVSPs) are hemostatically active toxins that perturb the maintenance and regulation of both the blood coagulation cascade and fibrinolytic feedback system at specific points, and hence, are widely used as tools in pharmacological and clinical diagnosis. The crystal structure of a thrombin-like enzyme (TLE) from *Bothrops jararacussu* venom (Jararacussin-I) was determined at 2.48 Å resolution. This is the first crystal structure of a TLE and allows structural comparisons with both the *Agkistrodon contortrix contortrix* Protein C Activator and the *Trimeresurus stejnegeri* plasminogen activator. Despite the highly conserved overall fold, significant differences in the amino acid compositions and three-dimensional conformations of the loops surrounding the active site significantly alter the molecular topography and charge distribution profile of the catalytic interface. In contrast to other SVSPs, the catalytic interface of Jararacussin-I is highly negatively charged, which contributes to its unique macromolecular selectivity.

Keywords: Jararacussin-I; thrombin-like enzyme; Bothrops jararacussu; crystal structure

Additional Supporting Information may be found in the online version of this article.

A. Ullah and T. A. C. B. Souza contributed equally to this work.

L. M. Zanphorlin's current address is Department of Chemistry, UNICAMP, Campinas, Brazil.

Grant sponsors: FAPESP, CNPq, TWAS, DAAD, CAPES.

*Correspondence to: Raghuvir Krishnaswamy Arni, Departamento de Física, Universidade Estadual Paulista (UNESP), São José do Rio Preto, 15054-000, SP, Brasil. E-mail: arni@sjrp.unesp.br

Introduction

Hemostasis, a complex, intricate, and highly regulated system, is primed and orchestrated by the necessity of maintaining the delicate balance between coagulation and fibrinolysis. The majority of the enzymes involved in this system belong to the serine proteinase superfamily, which include plasmin, kallikrein, urokinase-like plasminogen activator (uPA), tissue factor-like plasminogen activator (tPA), and the multi-functional enzyme, thrombin.¹ Thrombin can either stimulate coagulation or

suppress upstream events in the blood coagulation cascade by depleting factor Va.^{2–6}

Snake venoms are rich sources of hemostatically active toxins (HATs) that perturb both the blood coagulation cascade and fibrinolytic feedback system at specific points.⁷ HATs are typically, highly specific serine proteinases and rely on sophisticated molecular mechanisms, to activate or deplete coagulation factors such as fibrinogen (thrombin-like enzymes [TLEs]⁷), protein C (protein C activators⁹) and plasminogen (plasminogen activators⁸). Although TLEs such as the plasminogen and PC activators share significant sequence identity (50–70%), their high specificity toward different macromolecular targets results in different physiological responses in the hemostatic system.

Since snake venom TLEs share significant sequence identity with mammalian thrombin (around 30%) and the catalytic triad consisting of His57-Asp102-Ser195 is strictly conserved,¹¹ their amidolytic activity profiles and subsite specificities are similar. These enzymes are widely referred to as TLEs due to their ability to mimic the procoagulant activity of thrombin by catalyzing the hydrolysis of fibrinopeptides α or β (rarely both) from fibrinogen (factor I), resulting in the formation of a soft clot.^{11–14} TLEs are potentially relevant and possess therapeutical and clinical applications and those isolated from *Calloselasma rhodostoma* and *Bothrops atrox* are commercially available and are used for diagnosis and clinical tests.¹⁵ TLEs are clinically interesting and have been tested as defibrinogenating agents for the treatment of patients with severe cardiovascular disorders. To date, a number of TLEs have been functionally characterized from snake venoms^{7,15–27}; however none of their three-dimensional structures have been determined. So far, only a protein C activator and a plasminogen activator have been structurally characterized and the determination of a TLE structure represents an important step in order to delineate the structural and molecular basis for snake venom serine proteinases (SVSPs) selectivity.

Here, we describe the first snake venom TLE structure revealing a catalytic interface with a highly negative electrostatic potential, which probably contributes to the observed macromolecular selectivity in targeting the enzyme to fibrinogen.

Result and Discussion

The structure of Jararacussin-I was solved at 2.48 Å resolution (Table I) by molecular-replacement methods using the MOLREP program²⁸ and a model based on the atomic coordinates of the native protein C activator from the venom of *Agkistrodon contortrix contortrix* (ACC-C, PDB code: 2AIP).⁹

Jararacussin-I is comprised of 232 amino-acid residues folded in two domains each containing a

Table I. Data Collection and Refinement Statistics of Jararacussin-I

Data collection	
Beamline	W01B-MX2, LNLS
Wavelength (Å)	1.459
Space group	<i>I4</i>
Unit-cell parameters (Å)	<i>a</i> = <i>b</i> =84.53, <i>c</i> =80.24
Resolution range (Å)	50.00–2.48 (2.54–2.48)
No. of Unique reflections	8,484 (786)
Multiplicity ^a	3.8 (3.3)
Completeness (%)	96.9 (91.0)
$\langle I/\sigma(I) \rangle$	16.1 (3.3)
R_{merge}^b (%)	7.5 (33.9)
Matthews coefficient (Å ³ Da ⁻¹)	2.75
Corresponding solvent (%)	55.23
Model refinement	
Protein Data Bank ID	4GSO
Number of protein chains	1
Number of water molecules	22
R_{work}^c (%)	20.5
R_{free} (%)	24.4
R.m.s.d. from ideal bond lengths (Å)	0.03
R.m.s.d. from ideal angles (°)	1.36
Average <i>B</i> -factor (Å ²)	35.0
Ramachandran plot	
Most favored regions (%)	89.1
Allowed regions (%)	9.6
Disallowed regions (%)	1.3

^a Values for the outermost resolution shell are given in parentheses.

^b $R_{\text{merge}} = \frac{\sum_{hkl} \sum_i |I_i(hkl) - \langle I(hkl) \rangle|}{\sum_{hkl} \sum_i I_i(hkl)}$, where $I_i(hkl)$ is the intensity of the *i*th observation of reflection *hkl* and $\langle I(hkl) \rangle$ is the average over all observations of reflection *hkl*.

^c $R_{\text{work}} = \frac{\sum_{hkl} \|F_{\text{obs}} - F_{\text{calc}}\|}{\sum_{hkl} F_{\text{obs}}}$, where F_{obs} and F_{calc} are the observed and calculated structure-factor amplitudes, respectively. R_{free} is R_{work} calculated using 5% of the data that were omitted from refinement.

six-stranded β -barrel and one short α -helix. As expected, the tertiary structure is highly conserved among SVSPs such as ACC-C⁹ and TSV-PA (a plasminogen activator from *Trimeresurus stejnegeri* venom¹⁰) and structural overlays result in r.m.s.d.s of 1.21 Å and 0.81 Å, respectively. The main differences are located at the loops surrounding the active site [residues 20–24, 42–47 72–86, 122–136, and 154–161, Jararacussin-I numbering; Fig. 1(A)]. The amino acid sequences comprising these loops are unique to each snake venom serine proteinase (SVSP) [Fig. 1(B)] and generate different glycosylation and charge profiles around the active-site pocket. TSV-PA, ACC-C, and Jararacussin-I are often referred to as glycoproteins; however, the effects of glycosylation with respect to their specificities are distinct. Among the three glycosylation sites (N38, N96A, and N148) present in ACC-C, only the one at position N148 is conserved in Jararacussin-I [Fig. 1(A)]. TSV-PA contains a glycosylation site at N178¹⁰ that is not conserved in Jararacussin-I [Fig. 1(A)]. It has been shown that glycosylation has no effect on TSV-PA activity,²⁹ however in

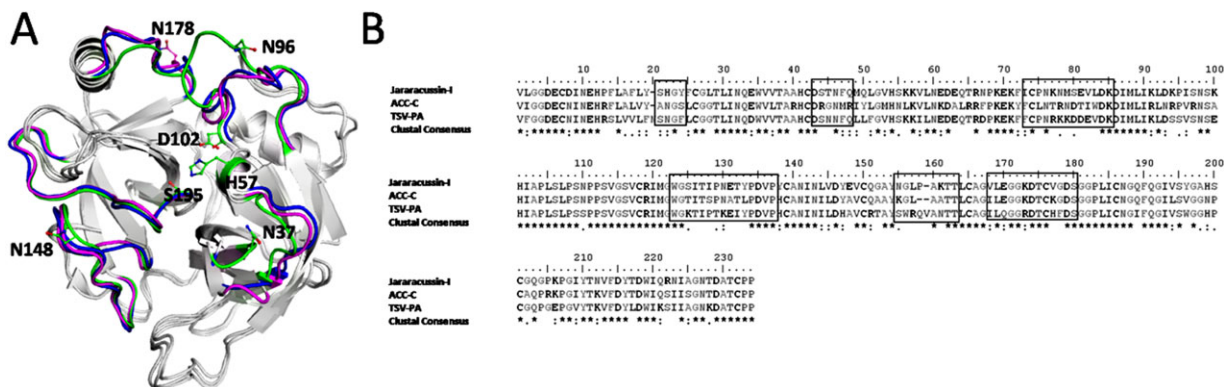


Figure 1. Sequence and structural comparisons of snake venom serine proteinases. A: Structural overlays of Jararacussin-I (loops in magenta), ACC-C (loops in green), and TSV-PA (loops in blue). The loops surrounding the active site, the catalytic triad (H57, D102, and S195), and the glycosylation sites in ACC-C (N37, N96, and N148) and TSV-PA (N178) are highlighted. B: Sequence alignment of Jararacussin-I, ACC-C, and TSV-PA. Boxed residues indicate loops surrounding the active site. [Color figure can be viewed in the online issue, which is available at wileyonlinelibrary.com.]

ACC-C, glycosylation plays a key role in macromolecular selectivity.⁹

Amino acid substitutions in the loops surrounding the active site significantly alter the surface charge distribution profile (Fig. 2) at the catalytic interface of Jararacussin-I in comparison to ACC-C and TSV-PA. Surface charge analysis demonstrated that Jararacussin-I exhibits a highly negatively charged surface around the active site [Fig. 2(A)], whereas in ACC-C the corresponding area is positively charged [Fig. 2(B)]. In addition, the differences in the loops surrounding the active site modifies the molecular topography of the catalytic interface, which along with the overall charge profile probably determines the macromolecular selectivity of Jararacussin-I.

The structural determinants for the mode of action of a plasminogen activator (TSV-PA, PDB ID: 1BQY) and a PC activator (ACC-C, PDB ID: 2AIP) have already been proposed by Parry *et al.*⁹ and Murakami and Arni,¹⁰ respectively. In TSV-PA, Phe 193 accounts for the high substrate specificity of TSV-PA and Asp97 is crucial for the plasminolytic activity. In ACC-C, the positive charge present on the interfacial surface and the carbohydrate moieties are important features that likely play crucial roles in PC recognition/binding/activation.

In this work, we postulate that the charge distribution profiles together with changes in the molecular topography around the catalytic interface are instrumental in defining macromolecular selectivity of TLEs.

Materials and Methods

Materials

Desiccated *B. jararacussu* crude venom (250 mg) was purchased from Serpentarium SANMARU, Taquaral, São Paulo, Brazil. Sephacryl S-100 16/60

and Benzamidine Sepharose 4 Fast Flow were obtained from GE Healthcare Life sciences. Molecular mass standards (GE Healthcare Life sciences) were bovine serum albumin (66 kDa); ovalbumin (44 kDa), carbonic anhydrase (30 kDa), soybean

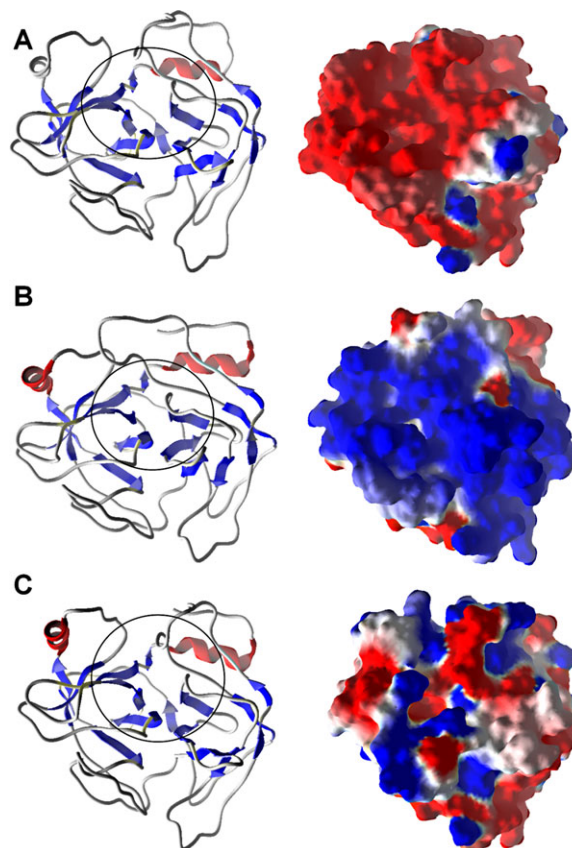


Figure 2. Surface charge distributions of Jararacussin-I (A), ACC-C (B), and TSV-PA (C), highlighting the contrasts at the catalytic interface. Black circles indicate the location of the active-site pocket. Red and blue represent negative and positive charges, respectively. [Color figure can be viewed in the online issue, which is available at wileyonlinelibrary.com.]

trypsin inhibitor (20.1 kDa), and α -lactalbumin (14.4 kDa). All the other reagents were from Sigma-Aldrich, Brazil.

Purification

Size-exclusion chromatography. About 125 mg of *B. jararacussu* crude venom was suspended in 1.5 mL of Tris-HCl buffer containing 0.02M Tris; 0.15M NaCl, pH 8.0 and centrifuged at 10,000g for 10 min. The clear supernatant was applied to a 16 × 60 cm Sephacryl S-100 column previously equilibrated with a 0.02M Tris-HCl pH 8.0 buffer containing 0.15M NaCl, the absorption was monitored at 280 nm [Supporting Information Fig. S1(A)]. All fractions were analyzed by sodium dodecyl sulfate polyacrylamide gel electrophoresis (SDS-PAGE) [Supporting Information Fig. S1(B)]. The above chromatographic procedure was repeated twice, totaling 250 mg of crude venom.

Affinity chromatography. The fractions containing Jararacussin-I from molecular exclusion chromatography was pooled (total volume of ~30 mL). This pool was applied to a benzamidine sepharose 4 fast flow column (high sub) (5 mL bed volume) using a super-loop at a flow rate of 0.5 mL/min. The column was pre-equilibrated with Tris-HCl 0.02M, NaCl 0.15M pH 8.0. The non-specifically bound proteins were eluted with the above buffer which additionally contained 0.5M NaCl. The specifically bound proteins were eluted by rapidly changing the pH from 8.0 to 3.0 using a glycine-HCl buffer. Proteins were eluted with a flow rate of 0.5 mL/min and fractions of 1 mL/tube were collected [Supporting Information Fig. S2(A)]. The pH of the eluted samples was immediately adjusted to pH 7.0 by adding a buffer containing 1M Tris pH 9.0. All fractions were analyzed by SDS-PAGE [Supporting Information Fig. S2(B)].

Crystallization. The Jararacussin-I sample was dialyzed against a 0.02M sodium acetate buffer pH 5.6 and was concentrated to 20 mg/mL in micro-concentrators (AMICON). Crystallization was performed by the hanging-drop vapor-diffusion method at 291 K using 24-well tissue-culture plates.³⁰ The crystallization screen kits used were, Crystal Screen, Crystal Screen 2, Grid Screen Ammonium sulfate, and Grid Screen PEG 6000 (Hampton Research) and PEG suite (Qiagen). Typically, 1 μ L drop of protein solution were mixed with 1 μ L of the screening solution and equilibrated over a reservoir containing 0.5 mL of the latter solution. Initially, micro-crystals were obtained with 0.1M 2-(N-morpholino)ethanesulfonic acid (MES) pH 6.5, 0.01M zinc sulfate, and 25% (wt/vol) polyethylene glycol monomethyl ether (PEG) 550 MME. These conditions were optimized by

changing the pH of the buffer and concentration of PEG and large single crystal were obtained when a 2 μ L protein droplet was mixed with an equal volume of the reservoir solution containing 0.1M MES pH 6.7 and 30% PEG 550 MME.

Data collection and structure determination

The TLE crystal from *B. jararacussu* was directly flash-frozen in a 100 K nitrogen-gas stream and X-ray diffraction data were collected on the W01B-MX2 beamline at the Brazilian Synchrotron Light Laboratory (Campinas, Brazil). The wavelength of the radiation source was set to 1.458 Å and a MarMosaic 225 mm CCD detector was used to record the X-ray diffraction intensities. The data were indexed, integrated, and scaled using the DENZO and SCALEPACK programs from the HKL-2000 package.³¹ Molecular replacement was carried out using the MOLREP²⁸ program and a model based on the atomic coordinates of native protein C activator from the venom of *Agkistrodon contortrix contortrix* (PDB code 2AIP).⁹

Acknowledgment

A. Ullah is the recipient of a TWAS doctoral fellowship.

References

1. Turgeon VL, Houenou LJ (1997) The role of thrombin-like (serine) proteases in the development, plasticity and pathology of the nervous system. *Brain Res Brain Res Rev* 25:85–95.
2. Baglia FA, Walsh PN (1998) Prothrombin is a cofactor for the binding of factor XI to the platelet surface and for platelet-mediated factor XI activation by thrombin. *Biochemistry* 37:2271–2281.
3. Alberio L, Dale GL (1999) Review article: platelet-collagen interactions: membrane receptors and intracellular signalling pathways. *Eur J Clin Invest* 29:1066–1076.
4. Oliver JA, Monroe DM, Church FC, Roberts HR, Hoffman M (2002) Activated protein C cleaves factor Va more efficiently on endothelium than on platelet surfaces. *Blood* 100:539–546.
5. Kini RM (2005) The intriguing world of prothrombin activators from snake venom. *Toxicon* 45:1133–1145
6. Monroe DM, Hoffman M (2012) The clotting system - a major player in wound healing. *Haemophilia* 18:11–16.
7. Tu AT (1991) *Handbook of natural toxins*. New York: Marcel Dekker.
8. Bortoleto RK, Murakami MT, Watanabe L, Soares AM, Arni RK (2002). Purification, characterization and crystallization of Jararacussin-I, a fibrinogen-clotting enzyme isolated from the venom of *Bothrops jararacussu*. *Toxicon* 40:1307–1312.
9. Murakami MT, Arni RK (2005). Thrombomodulin-independent activation of protein C and specificity of hemostatically active snake venom serine proteinases: crystal structures of native and inhibited *Agkistrodon contortrix contortrix* protein C activator. *J Biol Chem* 280:39309–39315.
10. Parry MA, Jacob U, Huber R, Wisner A, Bon C, Bode W (1998) The crystal structure of the novel snake venom plasminogen activator TSV-PA: a prototype

- structure for snake venom serine proteinases. *Structure (Camb.)* 6:1195–1206.
11. Barrett AJ, Rawlings ND (1995) Families and clans of serine peptidases. *Arch Biochem Biophys* 318:247–250.
 12. Aronson DL (1976) Comparison of the actions of thrombin and the thrombin-like venom enzymes ancrod and batroxobin. *Thromb Haemost* 36:9–13.
 13. Bell WR (1998) Clinical trials with Ancrod. In: Markland FS, (ed.), *Hemostasis and Animal Venoms*. Marcel Dekker, New York. pp 541–551.
 14. de Oliveira DG, Murakami MT, Cintra AC, Franco JJ, Sampaio SV, Arni RK (2009) Functional and structural analysis of two fibrinogen-activating enzymes isolated from the venoms of *Crotalus durissus terrificus* and *Crotalus durissus collilineatus*. *Acta Biochim Biophys Sin (Shanghai)* 41:21–29.
 15. Marsh N, Williams V (2005) Practical applications of snake venom toxins in haemostasis. *Toxicon* 45:1171–1181.
 16. Mandelbaum FR, Henriques OB (1964). Purification and properties of bothrops protease A. *Arch Biochem Biophys* 104:369–374.
 17. Stocker K, Barlow GH (1976) The coagulant enzyme from *Bothrops atrox* venom (batroxobin). *Methods Enzymol* 45:214–223.
 18. Kirby EP, Niewiarowski S, Stocker K, Kettner C, Shaw E, Brudzynski TM (1979) Thrombocytin, a serine protease from *Bothrops atrox* venom. I. Purification and characterization of the enzyme. *Biochemistry* 18:3564–3570.
 19. Itoh N, Tanaka N, Mihashi S, Yamashina I (1987) Molecular cloning and sequence analysis of cDNA for batroxobin, a thrombin-like snake venom enzyme. *J Biol Chem* 262:3132–3135.
 20. Hill-Eubanks DC, Parker CG, Lollar P (1989) Differential proteolytic activation of factor VIII-von Willebrand factor complex by thrombin. *Proc Natl Acad Sci USA* 86:6508–6512.
 21. Serrano SM, Sampaio CA, Mandelbaum FR (1993) Basic proteinases from *Bothrops moojeni* (caissaca) venom. II. Isolation of the metalloproteinase MPB. Comparison of the proteolytic activity on natural substrates by MPB, MSP 1 and MSP 2. *Toxicon* 31:483–492.
 22. Nishida S, Fujimura Y, Miura S, Ozaki Y, Usami Y, Suzuki M, Titani K, Yoshida E, Sugimoto M, Yoshioka A (1994) Purification and characterization of bothrobin, a fibrinogen-clotting serine protease from the venom of *Bothrops jararaca*. *Biochemistry* 33:1843–1849.
 23. Serrano SM, Mentele R, Sampaio CA, Fink E (1995) Purification, characterization, and amino acid sequence of a serine proteinase, PA-BJ, with platelet-aggregating activity from the venom of *Bothrops jararaca*. *Biochemistry* 34:7186–7193.
 24. Smolka MB, Marangoni S, Oliveira B, Novello JC (1998) Purification and partial characterization of a thrombin-like enzyme, balterobin, from the venom of *Bothrops alternatus*. *Toxicon* 36:1059–1063.
 25. Oliveira F, Rodrigues VM, Borges MH, Soares AM, Hamaguchi A, Giglio JR, Homs-Brandeburgo MI (1999) Purification and partial characterization of a new proteolytic enzyme from the venom of *Bothrops moojeni* (CAISSACA). *Biochem Mol Biol Int* 47:1069–1077.
 26. Petretski JH, Kanashiro M, Silva CP, Alves EW, Kipnis TL (2000) Two related thrombin-like enzymes present in *Bothrops atrox* venom. *Braz J Med Biol Res* 33:1293–1300.
 27. Costa Jde O, Fonseca KC, Mamede CC, Beletti ME, Santos-Filho NA, Soares A M, Arantes EC, Hirayama SN, Selistre-de-Araujo HS, Fonseca F (2010) Bhalternin: functional and structural characterization of a new thrombin-like enzyme from *Bothrops alternatus* snake venom. *Toxicon* 55:1365–1377.
 28. Vagin A, Teplyakov A (1997) MOLREP: an automated program for molecular replacement. *J Appl Crystallogr* 30:1022–1025.
 29. Zhang Y, Wisner A, Maroun RC, Choumet V, Xiong Y, Bon C (1997) Trimeresurus stejnegeri snake venom plasminogen activator. Site-directed mutagenesis and molecular modeling. *J Biol Chem* 272:20531–20537.
 30. Jancarik J, Kim SH (1991) Sparse matrix sampling: a screening method for crystallization of proteins *J Appl Crystallogr* 24:409–411.
 31. Otwinowski Z, Minor W (1997) Processing of X-ray diffraction data collected in oscillation mode. *Methods Enzymol* 276:307–326.